

Not All Neighbors Are Worth Attending to: Graph Selective Attention Networks for Semi-supervised Learning

Tiantian He^{1*}, Haicang Zhou^{2,3*}, Yew-Soon Ong^{1,2,3}, Gao Cong^{2,3}

¹Agency for Science, Technology and Research (A*STAR)

²Nanyang Technological University

³Singtel Cognitive and Artificial Intelligence Lab for Enterprises@NTU, Singapore

{He_Tiantian@ihpc.,Ong_Yew_Soon@hq.}a-star.edu.sg

{haicang001@e.,ASYSONg@gaocong@}ntu.edu.sg

ABSTRACT

Graph attention networks (GATs) are powerful tools for analyzing graph data from various real-world scenarios. To learn representations for downstream tasks, GATs generally attend to all neighbors of the central node when aggregating the features. In this paper, we show that a large portion of the neighbors are irrelevant to the central nodes in many real-world graphs, and can be excluded from neighbor aggregation. Taking the cue, we present Selective Attention (SA) and a series of novel attention mechanisms for graph neural networks (GNNs). SA leverages diverse forms of learnable node-node dissimilarity to acquire the scope of attention for each node, from which irrelevant neighbors are excluded. We further propose Graph selective attention networks (SATs) to learn representations from the highly correlated node features identified and investigated by different SA mechanisms. Lastly, theoretical analysis on the expressive power of the proposed SATs and a comprehensive empirical study of the SATs on challenging real-world datasets against state-of-the-art GNNs are presented to demonstrate the effectiveness of SATs.

CCS CONCEPTS

• Information systems → Data mining; • Computing methodologies → Neural networks.

KEYWORDS

Graph Attention, Graph Neural Networks, Semi-supervised Learning, Network Analysis

ACM Reference Format:

Tiantian He^{1*}, Haicang Zhou^{2,3*}, Yew-Soon Ong^{1,2,3}, Gao Cong^{2,3}, ¹Agency for Science, Technology and Research (A*STAR), ²Nanyang Technological University, ³Singtel Cognitive and Artificial Intelligence Lab for Enterprises@NTU, Singapore, {He_Tiantian@ihpc.,Ong_Yew_Soon@hq.}a-star.edu.sg, {haicang001@e.,ASYSONg@gaocong@}ntu.edu.sg. 2018. Not All Neighbors Are Worth Attending to: Graph Selective Attention Networks for Semi-supervised Learning. In *Proceedings of Make sure to enter the correct conference title from your rights confirmation email (Preprint)*. ACM, New York, NY, USA, 15 pages. <https://doi.org/XXXXXXX.XXXXXXX>

1 INTRODUCTION

Graph neural networks (GNNs) [1, 4, 13, 22–24, 33, 41, 45, 48, 49, 52, 53, 58] have achieved great success in semi-supervised learning tasks in graph-structured data. Among various types of GNNs, graph attention networks have gained popularity with multifarious real-world applications, especially arising from social and collaboration graphs [3, 10, 15, 32, 41, 43, 51, 56]. In each graph attention layer [41], the node representation is generally learned following a two-step procedure. Attention scores (attention coefficients) between each node and all its neighbors are firstly computed by some attention mechanism. The node representation for downstream tasks is then computed as a weighted aggregation of all neighbor features.

Existing GNNs typically include all neighbors in the scope (i.e., the receptive field) for feature aggregation [54]. However, it might not be always best to do so in attention-based GNNs (Fig. 1). Recent studies [36, 61] have shown that incorporating all neighbors in the scope for feature aggregation can possibly lead to deterioration in the predictive performances of GNNs on various graph learning tasks. Notably, our study also indicates that most neighbors in widely used social and collaboration graph datasets, such as Cora and Cite [38], are found to be far apart (see Appendix A for more details). This reveals that most neighbors in real-world graphs are highly dissimilar to the central node and are hence likely irrelevant for feature aggregation. Our idea is that adapting the scope of attention appropriately (i.e., the receptive field of graph attention for feature aggregation) can enable attention-based GNNs to learn better representations by attending more to highly relevant neighbors while ignoring the irrelevant ones. We conjecture that with better representations, the performance of GNNs on semi-supervised learning tasks would improve.

*Equal Contribution.

Permission to make digital or hard copies of all or part of this work for personal or classroom use is granted without fee provided that copies are not made or distributed for profit or commercial advantage and that copies bear this notice and the full citation on the first page. Copyrights for components of this work owned by others than ACM must be honored. Abstracting with credit is permitted. To copy otherwise, or republish, to post on servers or to redistribute to lists, requires prior specific permission and/or a fee. Request permissions from permissions@acm.org.

Preprint, Under review.

© 2018 Association for Computing Machinery.

ACM ISBN 978-x-xxxx-xxxx-x/YY/MM...\$15.00

<https://doi.org/XXXXXXX.XXXXXXX>

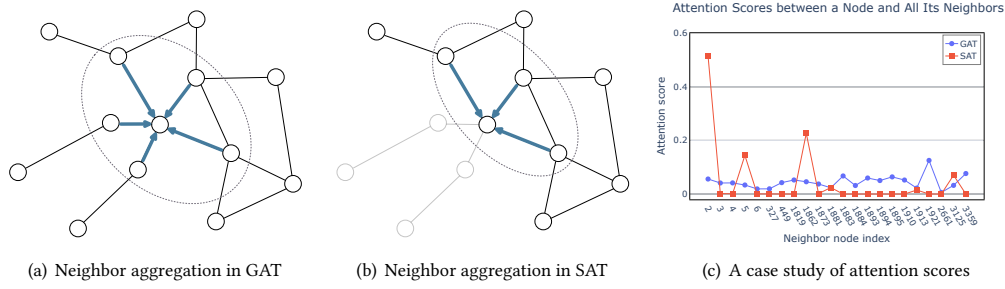


Figure 1: Schematic illustration of the difference between SAT and GAT. SAT (subfigure (b)) can learn the scope of attention for each node while GAT cannot (subfigure (a)). In subfigure (c), we exemplify the attention scores from a node and all its neighbors in a real-world dataset. Most of the learned attention scores learned by SAT are very close to 0, which means the corresponding neighbors are excluded from the feature aggregation. (Please refer to Section 5.4 for more details.)

Our present idea is inspired and motivated by studies [6, 9, 20] in cognitive science. Humans are known to be capable of determining the number of stimuli to respond to well, such as spoken words and presented images within their apprehension span [6]. The high quality of cognition is maintained by paying Selective Attention [9, 20] to the few stimuli identified in the apprehension span as most relevant to the cognitive goal, and ignoring the irrelevant ones. Although the idea of apprehension span has been tentatively adapted to solve some learning-based tasks in computer vision [18] and natural language processing [14, 30], how to adapt the scope of attention in attention-based GNNs for representation learning of graph data remains under-explored to date.

In this paper, we present an investigation on Graph selective attention networks that takes an analogy between the scope of attention for feature aggregation in GNNs and the apprehension span in human cognition. A series of Selective Attention (SA) mechanisms for graph neural networks is also proposed, and diverse forms of node-node dissimilarities for learning the node-wise scope of attention are investigated. Neighbors that are dissimilar to the central node based on the scope of attention are deemed as highly irrelevant, and hence excluded in the feature aggregation process. Our proposed SA mechanisms also return attention coefficients that are differentially pruned by the learned scope of attention, allowing highly irrelevant nodes to be ignored in feature aggregation. Subsequently, we propose and construct Graph selective attention networks (SATs) capable of learning effective representations that favor highly relevant nodes while ignoring the irrelevant ones (identified using the SA mechanisms). The main contributions of the paper are summarized as follows:

- We propose Selective Attention (SA), which comprises a class of novel attention mechanisms for GNNs. SA leverages node-node dissimilarity to learn the node-wise scope of attention, which can exclude irrelevant neighbors from the feature aggregation. SA thus endows GNNs with capabilities to learn representations that concentrate and aggregate features from highly relevant neighbors while ignoring irrelevant neighbors.
- The expressive power of the proposed SA layers is analyzed. The theoretical analysis verifies that the expressive power

of the proposed SA layers can reach the upper bound of all message-passing GNNs, indicating that SA layers are more powerful than those layers used in existing attention-based GNNs.

- We further use the proposed SA layers to construct Graph selective attention networks (SATs) for various downstream learning tasks arising from social and collaboration graphs. SATs are comprehensively tested on several well-established benchmarking datasets and compared to a number of state-of-the-art GNNs for the task of semi-supervised node classification and clustering. The results demonstrate that SATs can outperform other strong baselines.

2 RELATED WORK

Attention in GNNs. Graph attentions [3, 10, 12, 15, 25, 41, 42, 46] take advantage of effective attention mechanisms [5, 47] to dynamically learn the normalized node-node correlations regarding node features (attention scores/coefficients), which determine the neighbor importance for the subsequent feature aggregation. To further enhance the learning performance, there is a trend to inject graph structures into the computation of attention coefficients [8, 19, 31, 32, 51, 56]. Compared with existing attention-based GNNs, our method is fundamentally different. Our method can ignore irrelevant neighbors by considering diverse forms of dissimilarity between node pairs. Dissimilarity pertaining to graph structure is one possible choice of our approach. Besides, our experiments, which analyze the distribution of attention scores, show that injecting the graph structure into the computation of graph attention without considering the node-node dissimilarity cannot exclude those irrelevant neighbors from the feature aggregation.

Adjusting the scope of GNNs. In general, the scope (the receptive field) for each node in one GNN layer [54] is its first-order neighbors (including itself), and after k layers, it can capture the information from k -hop neighbors [3, 22, 41, 45]. There is a rich literature on carefully designing the scope for GNNs. This includes approaches (e.g., [4, 13, 26, 36, 55, 57]) that apply sampling strategies to improve the scalability of GNNs. Different from these methods, our work is not based on any sampling strategy. There are also some approaches [10, 61] adopting the top- k strategy to select the k most relevant

neighbors for aggregation. Unlike the top- k strategy, our method can learn how many neighbors to ignore for each node adaptively. In parallel, there have been several studies (e.g., [16, 27, 29, 49, 56, 60]) on designing adaptive receptive fields, either for each node [29] or for different parts of models [60]. To the best of our knowledge, none of these methods generate receptive fields by identifying and ignoring irrelevant neighbors.

3 GRAPH SELECTIVE ATTENTION NETWORKS

In this section, we introduce the proposed Graph selective attention networks (SATs). The Selective Attention layers adopting different Selective Attention mechanisms are firstly elaborated. How to use the proposed Selective Attention layers to construct SATs is then introduced. The computational complexity of SATs is finally analyzed.

3.1 Notations

Let $G = \{V, E\}$ denote a graph, where V and E represent the node and edge set. In G , there are N nodes, $|E|$ edges, and C classes ($C \ll N$) which the nodes possibly belong to. The adjacency matrix of G and the input node feature matrix are denoted as $A \in \{0, 1\}^{N \times N}$ and $X \in \mathbb{R}^{N \times D}$. Node i and its one-hop neighbors are denoted as \mathcal{N}_i . W^l and $\{h_i^l\}_{i=1, \dots, N}$ denote the learnable weight matrix and output representation of node i at l -th layer of SATs, respectively, and h^0 is set to be the input feature X .

3.2 Selective Attention layers

In this subsection, we present the Selective Attention (SA) layer, which is the core for building the Graph selective attention networks (SATs). The present graph attention mechanisms attempt to compute attention coefficients to all neighbors of each node. However, our preliminary study has shown that most neighbors in widely used graph datasets are quite irrelevant when evaluated by simple criteria (Appendix A). Thus, these irrelevant neighbors can be excluded from the neighbor aggregation in an appropriate way. Meanwhile, humans flexibly adjust the number of stimuli to respond in their apprehension span [6]. Specifically, in order to maintain the quality of cognition, human selectively attends to a few stimuli that are most relevant to the cognitive goal but ignores those irrelevant ones. Inspired by these, in this paper, we propose Selective Attention, which utilizes diverse forms of node-node dissimilarity to learn the scope of attention for each node. Irrelevant neighbors can be ignored in the feature aggregation stage. SA therefore endows SATs with the capability of learning representations concentrating on highly relevant neighbors.

Given a set of node features $\{h_i^l\}_{i=1, \dots, N}$, $h_i^l \in \mathbb{R}^{D^l}$, the Selective Attention layer maps them to D^{l+1} dimensional vectors $\{h_i^{l+1}\}_{i=1, \dots, N}$. The mapping requires weighted aggregation, with weights computed from both correlations of node features and diverse forms of node-node dissimilarity. The feature correlation between two connected nodes is firstly obtained. To generate the correlations of node features between connected nodes, we adopt

the method in [41]:

$$f_{ij} = \frac{\exp(\text{LeakyReLU}(a^T (W^l h_i^l \parallel W^l h_j^l)))}{\sum_{k \in \mathcal{N}_i} \exp(\text{LeakyReLU}(a^T (W^l h_i^l \parallel W^l h_k^l)))}, \quad (1)$$

where $a \in \mathbb{R}^{2D^{l+1}}$ is a vector of attention parameters, \parallel stands for the concatenation function for two vectors, and W^l is a $D^{l+1} \times D^l$ parameter matrix for feature mapping. Given f_{ij} computed from Eq. (1), the proposed SA layer can capture the feature correlations between connected nodes.

As mentioned above, existing graph attention mechanisms [3, 15, 41, 56] do not consider adjusting the scope of attention, resulting in somewhat less informative attention scores. To address this, the proposed Selective Attention further considers utilizing diverse forms of node-node dissimilarity to learn the scope of attention for each node in the graph. The node-node dissimilarity, which will be introduced later in this subsection, can quantify the extent that a neighbor can be ignored. Leveraging the aforementioned feature correlations (Eq. (1)) and node-node dissimilarity, we propose two different strategies derived from the SA concept to compute attention coefficients.

The first strategy is named as *Contractive apprehension span*, which is able to exponentially contract the normalized feature correlations (Eq.(1)). The attention score obtained via the *Contractive apprehension span* is defined as follows:

$$\alpha_{ij} = \frac{f_{ij} \cdot \exp(-\beta S_{ij})}{\sum_{k \in \mathcal{N}_i} f_{ik} \cdot \exp(-\beta S_{ik})}, \quad (2)$$

where S_{ij} represents the node-node dissimilarity, and $\beta \in (0, 1]$ is a positive hyperparameter used to control the significance of S_{ij} . As shown in Eq. (2), the feature-based attention scores are reduced as S_{ij} goes higher. The scope of attention for a given node is contracted as the attention coefficients obtained by Eq. (2) might be very close to zero. Those irrelevant neighbors can be less attended to in the feature aggregation according to S_{ij} , and the SA layer can therefore pay higher attention to those neighbors that are more relevant to the central node.

The second strategy is called *Subtractive apprehension span*. As its name implies, this strategy attempts to adjust the scope of attention by directly subtracting the effect brought by the dissimilarity between node pairs. The attention coefficient computed by the *Subtractive apprehension span* is defined as follows:

$$\alpha_{ij} = \frac{f_{ij}(1 - \beta T_{ij})}{\sum_{k \in \mathcal{N}_i} f_{ik}(1 - \beta T_{ik})}, T_{ij} = \frac{\exp(S_{ij})}{\sum_{k \in \mathcal{N}_i} \exp(S_{ik})}, \quad (3)$$

where $\beta \in (0, 1]$ is a positive hyperparameter controlling the effect of T_{ij} . Compared with the *Contractive apprehension span*, the above *Subtractive apprehension span* enables the SA layers to adjust the scope of the attention for feature aggregation in a more radical way, as some attention coefficients between connected nodes can be reduced to zero when T_{ij} is sufficiently high. *Subtractive apprehension span* allows SA layers to concentrate only on those relevant nodes when aggregating neighboring features for message passing in the GNN.

With the Selective Attention coefficients, the SA layer now can aggregate features associated with each node and its neighbors to generate layer outputs, which will be either propagated to the

higher layer, or be used as the representations for downstream tasks. The described aggregation phase can be formulated as follows:

$$h_i^{l+1} = (\alpha_{ii} + \epsilon \cdot \frac{1}{|N_i|}) W^l h_i^l + \sum_{j \in N_i, j \neq i} \alpha_{ij} W^l h_j^l, \quad (4)$$

where $\epsilon \in (0, 1)$ is a learnable parameter to improve the expressive power of the SA layer.

Node-node dissimilarity for Selective Attention. The proposed Selective Attention (SA) allows diverse node-node dissimilarity to be used to compute attention coefficients. In this paper, we use the following method to compute dissimilarity (S_{ij}) between each pair of connected nodes in the graph:

$$S_{ij} = \sum_k r_k \cdot \Psi_k(c_i^k, c_j^k), \text{ subject to } \sum_k r_k = 1, \quad (5)$$

where $\Psi(\cdot, \cdot)$ is a distance metric, k is the type index of dissimilarity, c_i^k is a vector characterizing node i from type k , and r_k is a learnable parameter used to balance the relative significance of different types of node properties, i.e., c_i^k . In this paper, we focus on two types of dissimilarity, which are node features (inputs) at each layer of the GNN and the structure of the nodes in the graph. By replacing $\Psi(\cdot, \cdot)$ as Euclidean distance function, Eq. (5) can be rewritten as:

$$S_{ij} = r_f \cdot \|Wh_i - Wh_j\|^2 + r_p \cdot \|p_i - p_j\|^2, \text{ subject to } r_f + r_p = 1, \quad (6)$$

where Wh_i is the features of node i in a GNN layer, and p_i is defined as a 1-by- C vector of node i in the latent space learned from graph structure. As p_i is assumed to be learnable, different learning approaches enable p_i to capture different properties in the graph structure. In this paper, we mainly consider the learnable properties hidden in the graph adjacency. Thus, we have:

$$L(P) = \arg \min_{PP^T} \sum_{i,j} (A_{ij} - [PP^T]_{ij})^2, \quad (7)$$

where P is an N -by- C matrix containing all p_i s. As shown in Eq. (7), P is learned by matrix factorization, which assumes that the edge adjacency matrix A can be reconstructed by PP^T . Through Eq. (7), similar nodes in the graph will induce a low distance in Eq. (6), and vice versa.

3.3 The architecture of Graph selective attention networks

Now, we can build Graph selective attention networks (SATs) with the proposed SA layers. "To stabilize the learning process", we follow [15, 40, 41] to use the multi-head attention strategy when constructing SATs. SATs either concatenate the node representations generated by multiple attention heads as the input of the next layers, or compute the mean of node features obtained by multiple attention heads as the output representations. As we in this paper additionally define learnable latent spaces for each node in the graph, the overall loss function for SATs is slightly different from classical graph attention networks. It is conceptually written as follows:

$$L = L_{task} + L(P), \quad (8)$$

where $L(P)$ is the MF method shown in Eq. (7), and L_{task} is the task-specific loss.

3.4 Computational complexity of Selective Attention layers

As each layer in SATs additionally requires node-node dissimilarity to compute Selective Attention coefficients, the computational complexity is slightly different from classical attention-based GNNs. Let D^l (or D^{l+1}) denote the dimension of the input (or output) vector of the l -th layer. The complexity of feature aggregation in the l -th layer is $O(ND^l D^{l+1} + (|E| + e)D^{l+1})$ for one attention head, where e represents the average degree of each node and N is the number of nodes in the input graph. This is the same as that of classical graph attention networks [41]. When there are K attention heads, the complexity is $O(KND^l D^{l+1} + K(|E| + e)D^{l+1})$. Additional computation in SATs is demanded as SATs have to capture node-node dissimilarity for the computation of Selective Attention coefficients. The complexity for learning the node-node dissimilarity in each attention head is $O(e(D^{l+1} + 2C))$, where C represents the dimension of each p in Eq. (6).

4 THEORETICAL ANALYSIS

In this section, the expressive power of the proposed SATs is analyzed. The expressive power evaluates whether a GNN can discriminate distinct (sub)structures wherein nodes have different features. Thus, it can theoretically reveal whether a GNN is sufficiently powerful for various downstream tasks. Recent studies [7, 48, 59] have shown that the feature aggregations in all message-passing GNNs are similar to the injective 1-dimensional Weisfeiler-Lehman test (1-WL test) [44]. Theoretically, the expressive power of all message-passing GNNs is as most as the 1-WL test [48].

As the proposed SATs belong to message-passing GNNs, their expressive power can be verified by showing the injectivity of the feature aggregation in SATs. To do so, we first prove that either *Contractive* (Eq. (2)), or *Subtractive apprehension span* (Eq. (3)) is still unable to distinguish some structures satisfying some conditions, without the improving term shown in Eq. (4), i.e., $\epsilon \cdot \frac{1}{|N_i|} W^l h_i^l$. Then, we prove that all the SA layers can discriminate all different structures when aggregating neighboring features utilizing either of the two proposed strategies integrated with $\epsilon \cdot \frac{1}{|N_i|} W^l h_i^l$ (Eq. (4)). Before the proof, we follow [15, 48] to give the notations for multisets. For the nodes in N_i , their feature vectors form a multiset $X_i = (M_i, \mu_i)$, where $M_i = \{s_1, \dots, s_n\}$ is the underlying set of X_i containing its *distinct elements*, and $\mu_i : M_i \rightarrow \mathbb{N}^*$ gives the multiplicity of each distinct element in M_i .

For the neighborhood aggregating function that is solely based on the *Contractive apprehension span* (Eq. (2)), the following theorem shows that it still cannot distinguish some structures.

THEOREM 4.1. *Let c_i denote the feature vector of node i , and $X_i = \{M_i, \mu_i\} \in \mathcal{X}$ denote a multiset comprising the features from nodes in N_i , where \mathcal{X} represents the countable feature space. The aggregation function using the attention scores computed by Eq. (2) is denoted as $h(c_i, X_i) = \sum_{x \in X_i} \alpha_{c_i x} g(x)$, where $g(\cdot)$ is a function defined on X_i and $\alpha_{c_i x}$ is the attention score between $g(c_i)$ and $g(x)$. For all g , any two nodes 1 and 2 and the Contractive apprehension span in Eq. (2), $h(c_1, X_1) = h(c_2, X_2)$ holds if and only if $c_1 = c_2, M_1 = M_2 = M$, and $q \cdot \sum_{y=x, y \in X_1} \psi(-\beta S_{c_1 y}) = \sum_{y=x, y \in X_2} \psi(-\beta S_{c_2 y})$, for $q > 0$ and $x \in M$, where $\psi(\cdot)$ is a function for mapping values to \mathbb{R}^+ .*

PROOF. Due to space limitations, here we briefly illustrate the method for completing the proof of Theorem 4.1. The full proof can be checked via https://anonymous.4open.science/r/WWW_2023_suppl-2D69/. The proof of Theorem 4.1 can be divided into two parts, i.e., the proof of the sufficiency and necessity of the iff conditions [15, 48, 59]. Given $c_1 = c_2$, $M_1 = M_2$, and $q \cdot \sum_{y=x, y \in X_1} \psi(-\beta S_{c_1 y}) = \sum_{y=x, y \in X_2} \psi(-\beta S_{c_2 y})$, $h(c_1, X_1) = h(c_2, X_2)$ can be easily verified. Thus, the sufficiency of the iff conditions stated in Theorem 4.1 is proved. Given $h(c_1, X_1) = h(c_2, X_2)$, the necessity of the iff conditions can be proved by showing possible contradictions when $M_1 \neq M_2$, $c_1 \neq c_2$, or $q \cdot \sum_{y=x, y \in X_1} \psi(-\beta S_{c_1 y}) \neq \sum_{y=x, y \in X_2} \psi(-\beta S_{c_2 y})$. \square

Theorem 4.1 shows that the function for feature aggregation (h) using the attention scores obtained by Eq. (2) may map different multisets into the same embedding if and only if these multisets share the same central node feature and the same node features whose node-node dissimilarity is proportional.

For the neighborhood aggregating function that is solely based on the *Subtractive apprehension span* (Eq. (3)), the following theorem shows that it cannot distinguish some structures.

THEOREM 4.2. *Given the same assumptions shown in Theorem 4.1 and the aggregation function using the attention scores computed by Eq. (3) is denoted as $h(c_i, X_i) = \sum_{x \in X_i} \alpha_{c_i x} g(x)$, for all g , any two nodes 1 and 2 and the Subtractive apprehension span in Eq. (3), $h(c_1, X_1) = h(c_2, X_2)$ holds if and only if $c_1 = c_2$, $M_1 = M_2 = M$, and $q \sum_{y=x, y \in X_1} [\sum_{x \in X_1} \psi(S_{c_1 x}) - \beta \psi(S_{c_1 y})] = \sum_{y=x, y \in X_2} [\sum_{x \in X_2} \psi(S_{c_2 x}) - \beta \psi(S_{c_2 y})]$, for $q > 0$ and $x \in M$, where $\psi(\cdot)$ is a function for mapping values to \mathbb{R}^+ .*

PROOF. The full proof of Theorem 4.2 can also be checked via https://anonymous.4open.science/r/WWW_2023_suppl-2D69/. \square

Theorem 4.2 shows that h solely based on Eq. (3) may map different multisets into the same embedding if and only if the multisets share the same central node feature, and the same node features whose adjusted negative dissimilarity is proportional. Theorems 4.1 and 4.2 show that the expressive power of SA layers solely utilizing *Contractive* (Eq. (2)) or *Subtractive apprehension span* (Eq. (3)) is stronger than that of classical graph attention networks [41], although they cannot discriminate some structures. As shown in the two presented theorems, the conditions giving rise to the failure of attention layers solely utilizing the *Contractive* or *Subtractive apprehension span* in distinguishing all structures are dependent on both node features and node-node dissimilarity. As node features and node-node dissimilarity are generally heterogeneous, it is infrequent for the conditions stated in Theorems 4.1 and 4.2 to be simultaneously satisfied. Such observation may well explain those attention-based GNNs additionally considering properties other than node features, e.g., injecting structural node embeddings [35] into the computation of attention coefficients can outperform classical graph attention networks.

However, the expressive power of SATs can be immediately improved to be equivalent to the 1-WL test through the slight modification as Eq. (4) shows. We next prove the proposed Selective Attention mechanisms (Eqs. (2) to (4)) can reach the upper bound of the expressive power of all message-passing GNNs by verifying

that the aggregation function based on Eq. (4) can successfully distinguish the structures whose properties meet the conditions stated in Theorems 4.1 and 4.2.

COROLLARY 4.3. *Assume \mathcal{T} is the attention-based aggregator shown in Eq. (4) and utilizes either Contractive (Eq. (2)) or Subtractive apprehension span (Eq. (3)), \mathcal{H} is a mapping of countable feature space X . \mathcal{T} operates on a multiset $H \in \mathcal{H}$. A \mathcal{H} exists so that with the attention-based aggregator in Eq. (4), \mathcal{T} can distinguish all different multisets that it previously cannot distinguish.*

PROOF. Corollary 4.3 can be proved by following the procedure presented in [15, 48]. According to Theorem 4.1, we assume $X_1 = (M, \mu_1)$, $X_2 = (M, \mu_2)$, $c \in M$, and $q \cdot \sum_{y=x, y \in X_1} \psi(-\beta S_{c_1 y}) = \sum_{y=x, y \in X_2} \psi(-\beta S_{c_2 y})$, for $q > 0$. When \mathcal{T} uses the attention scores solely according to Eq. (2) to aggregate node features, we have $\sum_{x \in X_1} \alpha_{cx} g(x) = \sum_{x \in X_2} \alpha_{cx} g(x)$. This means \mathcal{T} fails to discriminate the structures satisfying the conditions stated in Theorem 4.1. When \mathcal{T} uses Eq. (4) where the attention coefficients are obtained by the *Contractive apprehension span* (Eq. (2)) to aggregate node features, we have $\sum_{x \in X_1} \alpha_{cx} g(x) - \sum_{x \in X_2} \alpha_{cx} g(x) = \epsilon(\frac{1}{|X_1|} - \frac{1}{|X_2|}) \alpha_{cc} g(c)$, where $|X_1| = |\mathcal{N}_1|$, and $|X_2| = |\mathcal{N}_2|$. Since $|X_1| \neq |X_2|$, $\sum_{x \in X_1} \alpha_{cx} g(x) - \sum_{x \in X_2} \alpha_{cx} g(x) \neq 0$, which means \mathcal{T} based on Eqs. (2) and (4) is able to discriminate all the structures that \mathcal{T} solely based on Eq. (2) fails to distinguish. Following the similar procedure, when the Selective Attention layer (Eq. (4)) utilizes the *Subtractive apprehension span* (Eq. (3)), we are able to prove that the corresponding aggregation function also can distinguish those distinct structures that the aggregation function only using *Subtractive apprehension span* fails to discriminate. \square

Remarks. Based on the conducted theoretical analysis, the proposed SATs are the most powerful message-passing GNNs and are consequently more powerful than popular attention-based GNNs, e.g., GATs [41] and HardGAT [10]. In this paper, we mainly verify that the proposed Graph selective attention networks are the most powerful message-passing GNNs under the condition that the feature space is countable [15, 48, 59]. Recent studies have shown that a simplex operator for feature aggregations in some GNN layer is injective, i.e., the 1-WL test equivalent in the countable feature space [7]. But such injectivity might not hold when the simplex operator operates in the uncountable feature space. To ensure injectivity when a GNN deals with uncountable features, diverse forms of operators, e.g., mean, max, and min operators are required to collaboratively aggregate neighbor features. Thus, the expressive power of the proposed SATs can be equivalent to the 1-WL test in uncountable feature space by appropriately integrating with other effective operators for feature aggregation.

5 EXPERIMENT AND ANALYSIS

In this section, we evaluate the effectiveness of the proposed Selective Attention by comparing SATs with state-of-the-art approaches for two semi-supervised learning tasks on well-established benchmarking datasets. To understand the performance of SATs, we also perform ablation studies and visualize the distribution of learned attention coefficients. We also analyze the effect of β and the space consumption of SATs.

Table 1: Dataset statistics

Dataset	Type	Nodes	Edges	Features	Classes
Cora	Citation	2,708	5,429	1,433	7
Cite	Citation	3,327	4,552	3,703	6
Pubmed	Citation	19,717	44,324	500	3
Wiki	Web	2,405	17,981	4,973	17
Uai	Web	3,363	33,300	4,971	19
CoauthorCS	Collaboration	18,333	327,576	6,805	15

5.1 Experimental set-up

Baselines. SATs are compared with twelve strong baselines, including MoNet [33], GCN [22], GraphSage [13], JKNet [49], APPNP [23], ARMA [2], GIN [48], Neural Sparse [61], GAT [41], GATv2 [3], CAT [15], and HardGAT [10]. MoNet, GCN, JKnet, APPNP, and ARMA are five representative GNNs that leverage graph convolutional operators to learn representations. GIN and CAT are two state-of-the-art GNNs whose expressive power is equivalent to the 1-WL test. GAT and GATv2 are two powerful attention-based GNNs that learn representations by attending to all neighbors of each node in the graph. GraphSage, Neural Sparse, and HardGAT are three state-of-the-art GNNs that perform graph learning tasks by aggregating the features from sampled neighbors. By comparing with diverse types of GNNs which consider different scopes of neighbors for feature aggregation, the effectiveness of the proposed SATs can be better validated.

Datasets. Six widely used datasets, including Cora, Cite, Pubmed [28, 38], Wiki [28], Uai [28], and CoauthorCS [39] are used for evaluation. Cora, Cite, and Pubmed are citation networks widely used for the evaluation of GNNs. However, recent studies show that they may be insufficient to evaluate the performance of GNNs due to their limited data size [17, 39]. By following previous work, we additionally include Wiki, Uai, and CoauthorCS in our experiments. The data statistics are summarized in Table 1, and more details can be found in Appendix B.1.

Evaluation and experimental settings. Following previous work [15, 22, 24, 41], we mainly consider two learning tasks to test the effectiveness of different approaches, i.e., semi-supervised node classification and semi-supervised node clustering. For the training and testing paradigms, we closely follow the established settings reported in the previous studies [15, 22, 23, 41, 50]. The classification and clustering performances of all approaches are evaluated by *Accuracy*. In the training phase, all the GNNs are implemented with the two-layer network structure, i.e., one hidden layer followed by the output layer. All approaches are run 10 times on each testing dataset to obtain the average performance. We report the detailed experimental settings in Appendix B.2.

5.2 Results of semi-supervised learning

Semi-supervised node classification and clustering are closely related to several important applications from real-world graph data, such as social community detection and document classification. In our experiments, we use the proposed SATs to perform these two learning tasks in the aforementioned real graph datasets and

compare their performance with that of state-of-the-art GNNs. The corresponding results are summarized in Tables 2 and 3.

The performance comparisons of semi-supervised node classification are presented in Table 2. As the table shows, SATs consistently outperform all the baselines on all the datasets. Specifically, SAT archives 0.76%, 0.72%, 0.56%, 2.81%, 0.89%, and 0.69% improvement over the best baselines (which are underlined in Table 2) in terms of *Accuracy*. It is worth noting that SAT achieves significant performance gain over all attention-based GNNs. Specifically, SAT archives 0.76%, 0.72%, 0.75%, 3.11%, 9.35% and 0.69% performance gain over the best attention-based GNNs. The better performance of SATs could be attributed to its ability of identifying irrelevant neighbors and only attending to those highly relevant ones. This is why the performance improvement of SATs over attention-based GNNs is much more significant on Wiki, Uai, and CoauthorCS, where the density of edges is higher and more irrelevant neighbors exist. We will visualize the distribution of attention scores learned by SATs in Section 5.4 to demonstrate their ability to identify and ignore irrelevant neighbors.

The results of semi-supervised clustering are summarized in Table 3. SAT archives the best scores on five datasets, and it outperforms all the attention-based methods on all six datasets. Specifically, SAT archives 0.48%, 0.84%, 0.26%, 2.57%, 6.98%, 0.40% performance gain over the best attention-based GNN. Similar to the results on the first task, the *Accuracy* increases reported by SAT over attention-based GNNs are more significant on dense graphs, including Wiki, Uai, and CoauthorCS.

5.3 Ablation studies

To further investigate the effectiveness of our model, we conduct ablation studies on the two types of dissimilarity (Eq. (6)) of SAT. We consider vanilla GAT, SAT with dissimilarity only regarding node features (C/S-F) (i.e. $r_f = 1, r_p = 0$ in Eq. (6)), SAT with the dissimilarity of graph structure only (C/S-P) (i.e. $r_f = 0, r_p = 1$ in Eq. (6)), and the complete SAT model. The results of semi-supervised node classification and clustering tasks are summarized in Tables 4 and 5. From the tables, we observe that either using node features or node structural properties to compute node-node dissimilarity can improve the performances of graph attention, which demonstrates that ignoring irrelevant neighbors in graph attention indeed improves the performance. Meanwhile, considering both dissimilarities produces better and more stable results.

5.4 Visualization of attention scores

To demonstrate the ability of SA to ignore irrelevant neighbors, we compare the attention scores obtained by the output layer of GAT, CAT, and SATs. Here we show the results on Uai and the results on the other datasets are given in Appendix B.3. In Fig. 2, we conduct a case study on a node to show how SA mechanisms influence the values of attention coefficients of neighbors, and then we show the histogram of all attention scores. We observe that some attention scores obtained by SAT are close to zero, showcasing that SAT indeed can learn the scope of attention to exclude the irrelevant neighbors from the feature aggregation. Such observation generalizes to the whole graph, as the histogram of attention scores (Fig. 2) shows that more attention scores acquired by SAT are close

Table 2: Performance comparison on semi-supervised node classification. The results in bold show that SAT outperforms all the baselines and the best baselines are underlined.

Models	Cora	Cite	Pubmed	Wiki	Uai	CoauthorCS
MoNet	80.93 \pm 0.41	67.54 \pm 0.69	80.06 \pm 0.55	68.36 \pm 0.27	53.58 \pm 0.26	87.86 \pm 0.35
GCN	81.79 \pm 0.21	71.83 \pm 0.72	79.80 \pm 0.31	66.99 \pm 0.15	<u>60.72</u> \pm 0.23	88.50 \pm 1.06
JKNet	78.70 \pm 0.45	66.30 \pm 0.16	79.73 \pm 0.04	63.86 \pm 0.19	54.08 \pm 0.84	87.66 \pm 1.02
APPNP	82.50 \pm 0.42	72.04 \pm 0.48	<u>82.76</u> \pm 0.37	66.94 \pm 0.20	52.74 \pm 0.34	88.46 \pm 0.21
ARMA	80.47 \pm 0.71	69.45 \pm 0.57	76.63 \pm 0.56	66.94 \pm 0.17	54.56 \pm 0.15	82.18 \pm 0.37
GIN	81.27 \pm 0.57	66.30 \pm 0.59	80.37 \pm 0.69	<u>71.94</u> \pm 0.27	57.26 \pm 0.16	82.94 \pm 0.21
GAT	83.72 \pm 0.78	70.48 \pm 0.39	81.17 \pm 0.49	66.12 \pm 0.14	54.02 \pm 0.09	87.44 \pm 0.55
GATv2	84.06 \pm 0.83	71.44 \pm 0.45	81.94 \pm 0.29	66.82 \pm 0.41	56.02 \pm 0.21	87.84 \pm 0.11
CAT	<u>84.38</u> \pm 0.25	72.08 \pm 0.70	82.60 \pm 0.27	71.73 \pm 0.38	54.48 \pm 0.52	<u>90.71</u> \pm 0.21
HardGAT	79.44 \pm 0.52	<u>72.14</u> \pm 0.44	81.00 \pm 0.29	60.22 \pm 0.21	46.82 \pm 0.15	86.30 \pm 0.62
GraphSage	81.36 \pm 0.44	70.50 \pm 0.66	79.28 \pm 0.26	68.04 \pm 0.21	57.44 \pm 0.19	89.96 \pm 0.97
Neural Sparse	83.33 \pm 0.18	71.50 \pm 0.22	81.07 \pm 0.21	68.77 \pm 0.11	46.40 \pm 0.22	88.07 \pm 0.74
SAT-C	85.02 \pm 0.35	72.40 \pm 0.28	83.16 \pm 0.10	73.96 \pm 0.35	61.26 \pm 0.71	91.34 \pm 0.26
SAT-S	84.66 \pm 0.23	72.66 \pm 0.23	83.22 \pm 0.15	72.96 \pm 0.38	58.88 \pm 0.66	90.54 \pm 0.39

Table 3: Performance comparison on semi-supervised node clustering. The results in bold show that SAT outperforms all the baselines and the best baselines are underlined.

Models	Cora	Cite	Pubmed	Wiki	Uai	CoauthorCS
MoNet	79.06 \pm 0.61	63.35 \pm 0.29	79.78 \pm 0.40	71.68 \pm 0.14	55.21 \pm 0.31	87.52 \pm 0.92
GCN	74.61 \pm 0.24	63.61 \pm 0.80	77.56 \pm 0.56	72.78 \pm 0.51	60.14 \pm 0.18	88.72 \pm 0.73
JKNet	76.94 \pm 0.48	64.33 \pm 0.02	79.53 \pm 0.47	67.90 \pm 0.17	57.15 \pm 0.09	87.89 \pm 0.48
APPNP	80.44 \pm 0.94	70.33 \pm 0.62	<u>82.53</u> \pm 0.45	69.71 \pm 0.19	53.63 \pm 0.40	88.68 \pm 0.39
ARMA	77.99 \pm 0.91	68.07 \pm 0.89	78.01 \pm 0.98	71.28 \pm 0.12	58.44 \pm 0.13	82.43 \pm 0.33
GIN	79.59 \pm 0.36	66.04 \pm 0.83	78.39 \pm 0.88	<u>74.18</u> \pm 0.15	<u>60.39</u> \pm 0.11	85.34 \pm 0.29
GAT	<u>81.46</u> \pm 0.26	68.49 \pm 0.26	81.30 \pm 0.17	70.52 \pm 0.13	56.45 \pm 0.64	88.00 \pm 0.36
GATv2	80.79 \pm 0.54	70.03 \pm 0.36	81.43 \pm 0.17	69.10 \pm 0.17	57.47 \pm 0.22	88.13 \pm 0.56
CAT	81.13 \pm 0.24	<u>70.35</u> \pm 0.33	82.07 \pm 0.16	73.29 \pm 0.37	56.11 \pm 0.41	<u>90.48</u> \pm 0.22
HardGAT	76.53 \pm 0.36	69.68 \pm 0.44	79.89 \pm 0.18	63.19 \pm 0.18	47.65 \pm 0.15	87.32 \pm 0.55
GraphSage	78.50 \pm 0.67	68.92 \pm 0.42	79.74 \pm 0.49	70.72 \pm 0.70	59.77 \pm 0.11	89.97 \pm 0.43
Neural Sparse	80.69 \pm 0.24	69.97 \pm 0.19	80.79 \pm 0.04	71.19 \pm 0.35	50.98 \pm 0.20	88.38 \pm 0.44
SAT-C	81.85 \pm 0.27	70.82 \pm 0.19	82.28 \pm 0.09	75.17 \pm 0.31	61.48 \pm 0.61	90.84 \pm 0.21
SAT-S	81.47 \pm 0.21	70.94 \pm 0.09	82.22 \pm 0.07	74.05 \pm 0.38	59.31 \pm 0.55	90.29 \pm 0.09

Table 4: Ablation study in semi-supervised node classification

SAT (Contractive apprehension span)								
Dissimilarity node feature node structure		Models	Cora	Cite	Pubmed	Wiki	Uai	CoauthorCS
✓	✓	GAT	83.84	70.36	81.50	66.12	54.02	87.44
		C-F	83.87	72.00	82.17	71.70	60.17	90.77
		C-P	84.37	72.60	82.70	73.50	59.13	89.93
✓	✓	SAT-C	85.02	72.40	83.16	73.96	61.26	91.34
SAT (Subtractive apprehension span)								
Dissimilarity node feature node structure		Models	Cora	Cite	Pubmed	Wiki	Uai	CoauthorCS
✓	✓	GAT	83.84	70.36	81.50	66.12	54.02	87.44
		S-F	84.30	72.40	82.07	72.70	59.13	90.20
		S-P	84.13	72.60	82.50	73.17	56.97	90.17
✓	✓	SAT-S	84.66	72.66	83.22	72.96	58.88	90.54

Table 5: Ablation study in semi-supervised node clustering

SAT (Contractive apprehension span)								
Dissimilarity node feature	Dissimilarity node structure	Models	Cora	Cite	Pubmed	Wiki	Uai	CoauthorCS
√	√	GAT	81.39	69.20	80.88	70.52	56.45	88.00
		C-F	80.07	70.61	82.01	72.69	59.95	90.48
		C-P	81.18	70.80	82.25	74.39	59.37	89.78
√	√	SAT-C	81.85	70.82	82.28	75.17	61.48	90.84
SAT (Subtractive apprehension span)								
Dissimilarity node feature	Dissimilarity node structure	Models	Cora	Cite	Pubmed	Wiki	Uai	CoauthorCS
√	√	GAT	81.39	69.20	80.88	70.52	56.45	88.00
		S-F	81.08	70.99	81.98	73.24	59.36	90.14
		S-P	81.21	70.73	82.23	74.01	56.72	89.98
√	√	SAT-S	81.47	70.94	82.22	74.05	59.31	90.29

to zero compared with GAT and SAT. We also conduct the case study on CAT [15], which utilizes both node features and graph

structure to compute attention coefficients for graph analysis, and draw the distribution of its attention scores. We do not observe a significant difference in the histogram of attention scores between CAT and GAT, showing that CAT is not able to ignore irrelevant neighbors.

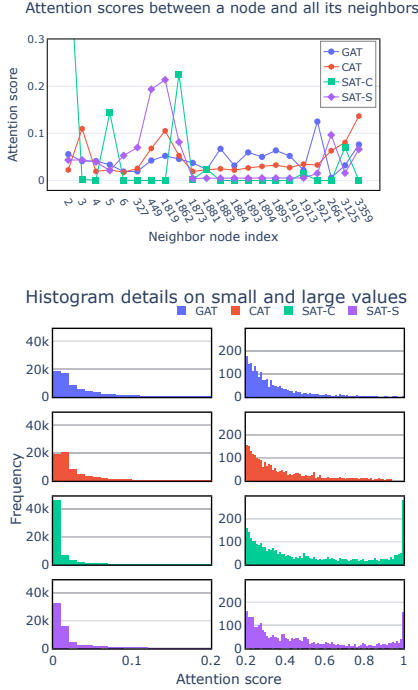


Figure 2: Attention scores from GAT, CAT and SATs on Uai

5.5 The effect of β

SATs use β to control the influence from the node-node dissimilarity when computing attention coefficients. The effect of the node-node dissimilarity becomes larger when β goes high. Potentially, SATs can learn smaller scopes of attention, which exclude more neighbors when β is set to high values. To show this, in Table 6, we list the number of edges with small attention scores (< 0.05) when β ranges in $[0.1, 0.5, 0.75, 1.0]$ on all testing datasets. As seen in the table, more neighbors are assigned with very small attention scores as β goes higher.

We show the *Accuracy* of our models with varying values of β in the range of $[0.01, 1.0]$ in Fig. 3. Based on the results in Table 6 and Fig. 3, one possible way to find a better setting of β is to configure it according to the density of the graph. Generally, SATs can perform better when β is set to a higher value in dense graphs, such as Wiki, Uai, and CoauthorCS. In these graphs, SATs can identify a large number of dissimilar neighbors as irrelevant to the feature aggregation, so that they can learn representations by concentrating on the features of a few relevant nodes. However, in sparse graphs such as Cora, Cite, and Pubmed, SATs can perform better when a

relatively small β is used. In these graphs, the number of neighbors connecting each central node is small. Thus, SATs do not need to identify many neighbors as irrelevant ones.

Table 6: The number of neighbors with very low attention coefficients (≤ 0.05) and proportions

Dataset	C: Contractive S: Subtractive	$\beta = 0.1$	$\beta = 0.5$	$\beta = 0.75$	$\beta = 1$
Cora	C	2273 (0.171)	2672 (0.201)	2726 (0.206)	2800 (0.211)
	S	2147 (0.162)	2164 (0.164)	2214 (0.167)	2415 (0.182)
Cite	C	879 (0.071)	1018 (0.082)	1081 (0.087)	1120 (0.090)
	S	878 (0.071)	897 (0.072)	902 (0.073)	1047 (0.084)
Pubmed	C	32416 (0.299)	34078 (0.314)	34590 (0.319)	35079 (0.324)
	S	32185 (0.297)	32268 (0.298)	32822 (0.303)	34809 (0.321)
Wiki	C	15870 (0.619)	16153 (0.6310)	16190 (0.632)	16663 (0.651)
	S	15944 (0.622)	15997 (0.625)	16006 (0.625)	16308 (0.637)
Uai	C	58699 (0.839)	58733 (0.839)	59726 (0.853)	62155 (0.888)
	S	62705 (0.896)	62741 (0.896)	62834 (0.898)	63688 (0.910)
CoauthorCS	C	79384 (0.436)	79838 (0.438)	79898 (0.439)	87610 (0.481)
	S	78909 (0.433)	78992 (0.434)	79857 (0.438)	80952 (0.444)

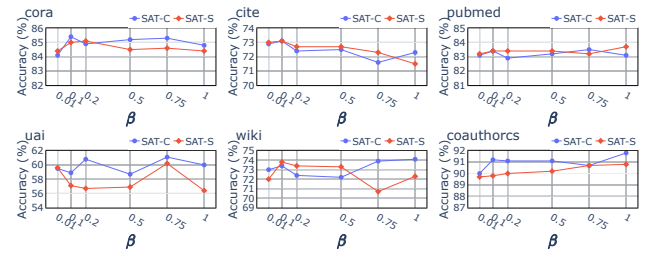


Figure 3: Sensitivity test for β .

5.6 Comparisons on model parameters and space consumption between GAT and SATs

To show the difference in architecture between GAT and SATs, we compare the number of parameters and memory usage between them. The results have been summarized in Table 7. SATs use slightly more memory since more parameters, which are mainly due to the learning of latent spaces (i.e., p), are used to perform the task of representation learning. Thus, SATs use slightly more memory in the training stage.

6 CONCLUSION

In this paper, we have proposed Selective Attention (SA), which generalizes a class of novel attention mechanisms for GNNs. Motivated by the analogy between the apprehension span of human cognition and the scope of attention for feature aggregation, SA leverages diverse forms of node-node dissimilarity to adapt the node-wise scope of attention, which can flexibly exclude those irrelevant neighbors

Table 7: Parameter comparison between GAT and SAT.

		Cora	Cite	Pubmed	Wiki	Uai	CoauthorCS
GAT	# Parameters	92430	237644	32454	2682658	2682150	3620126
	Space consumption	1.1GB	1.2GB	1.2GB	1.2GB	1.3GB	1.8GB
SAT-C	# Parameters	111285	257505	91504	2723058	2745562	3894636
	Space consumption	1.2GB	1.2GB	1.4GB	1.4GB	1.5GB	2.5GB
SAT-S	# Parameters	111285	257505	91504	2723058	2745562	3894636
	Space consumption	1.2GB	1.2GB	1.4GB	1.4GB	1.6GB	2.7GB

from the feature aggregation stage. SA therefore enables GNNs to learn representations by favoring the features of highly relevant neighbors and ignoring irrelevant neighbors. Given different SA mechanisms, we build Graph selective attention networks (SATs) to learn representations for various tasks arising from real-world graph data. SATs have been tested on widely used benchmarking datasets and compared to several strong baselines. The obtained notable results can validate the effectiveness of the proposed Selective Attention. In the future, the proposed SA will be further improved by exploring more forms of node-node dissimilarity that can be used for computing SA coefficients and developing SA mechanisms that are compatible with multi-view graphs.

REFERENCES

- [1] Sami Abu-El-Haija, Bryan Perozzi, Amol Kapoor, Nazanin Alipourfard, Kristina Lerman, Hrayr Harutyunyan, Greg Ver Steeg, and Aram Galstyan. 2019. Mixhop: Higher-order graph convolutional architectures via sparsified neighborhood mixing. In *ICML*. PMLR, 21–29.
- [2] Filippo Maria Bianchi, Daniele Grattarola, Lorenzo Livi, and Cesare Alippi. 2022. Graph neural networks with convolutional arma filters. *IEEE TPAMI* 44 (2022), 3496–3507.
- [3] Shaked Brody, Uri Alon, and Eran Yahav. 2021. How Attentive are Graph Attention Networks?. In *ICLR*.
- [4] Jianfei Chen, Jun Zhu, and Le Song. 2018. Stochastic Training of Graph Convolutional Networks with Variance Reduction. In *ICML*, Vol. 80. 941–949.
- [5] Jianpeng Cheng, Li Dong, and Mirella Lapata. 2016. Long Short-Term Memory Networks for Machine Reading. In *EMNLP*. 551–561.
- [6] Michelene TH Chi and David Klahr. 1975. Span and rate of apprehension in children and adults. *Journal of experimental child psychology* 19, 3 (1975), 434–439.
- [7] Gabriele Corso, Luca Cavalleri, Dominique Beaini, Pietro Liò, and Petar Veličković. 2020. Principal neighbourhood aggregation for graph nets. In *NeurIPS*, Vol. 33. 13260–13271.
- [8] Vijay Prakash Dwivedi and Xavier Bresson. 2020. A generalization of transformer networks to graphs. *arXiv preprint arXiv:2012.09699* (2020).
- [9] Di Fu, Cornelius Weber, Guochun Yang, Matthias Kerzel, Weizhi Nan, Pablo Barros, Haiyan Wu, Xun Liu, and Stefan Wermter. 2020. What can computational models learn from human selective attention? A review from an audiovisual unimodal and crossmodal perspective. *Frontiers in Integrative Neuroscience* 14 (2020), 10.
- [10] Hongyang Gao and Shuiwang Ji. 2019. Graph Representation Learning via Hard and Channel-Wise Attention Networks. In *KDD*. 741–749.
- [11] Xavier Glorot and Yoshua Bengio. 2010. Understanding the difficulty of training deep feedforward neural networks. In *AISTATS*, Vol. 9. 249–256.
- [12] Caglar Gulcehre, Misha Denil, Mateusz Malinowski, Ali Razavi, Razvan Pascanu, Karl Moritz Hermann, Peter Battaglia, Victor Bapst, David Raposo, Adam Santoro, et al. 2019. Hyperbolic Attention Networks. In *ICLR*.
- [13] William L. Hamilton, Zitao Ying, and Jure Leskovec. 2017. Inductive Representation Learning on Large Graphs. In *NeurIPS*. 1024–1034.
- [14] Wei Han, Hui Chen, Zhen Hai, Soujanya Poria, and Lidong Bing. 2022. SANCL: Multimodal Review Helpfulness Prediction with Selective Attention and Natural Contrastive Learning. In *COLING*.
- [15] Tiantian He, Yew-Soon Ong, and Lu Bai. 2021. Learning Conjoint Attentions for Graph Neural Nets. In *NeurIPS*, Vol. 34. 2641–2653.
- [16] Yifan Hou, Jian Zhang, James Cheng, Kaili Ma, Richard T. B. Ma, Hongzhi Chen, and Ming-Chang Yang. 2020. Measuring and Improving the Use of Graph Information in Graph Neural Networks. In *ICLR*.
- [17] Weihua Hu, Matthias Fey, Marinka Zitnik, Yuxiao Dong, Hongyu Ren, Bowen Liu, Michele Catasta, and Jure Leskovec. 2020. Open Graph Benchmark: Datasets for Machine Learning on Graphs. In *NeurIPS*.
- [18] Yifei Huang, Xiaoxiao Li, Lijin Yang, Lin Gu, Yingying Zhu, Hirofumi Seo, Qiuming Meng, Tatsuya Harada, and Yoichi Sato. 2021. Leveraging Human Selective Attention for Medical Image Analysis with Limited Training Data. In *BMVC*.
- [19] Md Shamim Hussain, Mohammed J Zaki, and Dharmashankar Subramanian. 2022. Edge-augmented graph transformers: Global self-attention is enough for graphs. In *KDD*.
- [20] William A Johnston and Veronica J Dark. 1986. Selective attention. *Annual review of psychology* 37, 1 (1986), 43–75.
- [21] Diederik P Kingma and Jimmy Ba. 2014. Adam: A method for stochastic optimization. *arXiv preprint arXiv:1412.6980* (2014).
- [22] Thomas N. Kipf and Max Welling. 2017. Semi-Supervised Classification with Graph Convolutional Networks. In *ICLR*.
- [23] Johannes Klicpera, Aleksandar Bojchevski, and Stephan Günnemann. 2019. Predict then Propagate: Graph Neural Networks meet Personalized PageRank. In *ICLR*.
- [24] Johannes Klicpera, Stefan Weissenberger, and Stephan Günnemann. 2019. Diffusion Improves Graph Learning. In *NeurIPS*. 13333–13345.
- [25] Devin Kreuzer, Dominique Beaini, Will Hamilton, Vincent Létourneau, and Prudencio Tossou. 2021. Rethinking graph transformers with spectral attention. In *NeurIPS*, Vol. 34.
- [26] Hongkang Li, Meng Wang, Sijia Liu, Pin-Yu Chen, and Jinjun Xiong. 2022. Generalization Guarantee of Training Graph Convolutional Networks with Graph Topology Sampling. In *ICML*, Vol. 162. 13014–13051.
- [27] Ziqi Liu, Chaochao Chen, Longfei Li, Jun Zhou, Xiaolong Li, Le Song, and Yuan Qi. 2019. GeniePath: Graph Neural Networks with Adaptive Receptive Paths. In *AAAI*. 4424–4431.
- [28] Qing Lu and Lise Getoor. 2003. Link-based Classification. In *ICML*, Tom Fawcett and Nina Mishra (Eds.). 496–503.
- [29] Xiaojun Ma, Junshan Wang, Hanyue Chen, and Guojie Song. 2021. Improving Graph Neural Networks with Structural Adaptive Receptive Fields. In *WWW*. 2438–2447.
- [30] Sameen Maruf, André F. T. Martins, and Gholamreza Haffari. 2019. Selective Attention for Context-aware Neural Machine Translation. In *NAACL-HLT*. 3092–3102.
- [31] Grégoire Mialon, Dexiong Chen, Margot Selosse, and Julien Mairal. 2021. Graphit: Encoding graph structure in transformers. *arXiv preprint arXiv:2106.05667* (2021).
- [32] Erxue Min, Runfa Chen, Yatao Bian, Tingyang Xu, Kangfei Zhao, Wenbing Huang, Peilin Zhao, Junzhou Huang, Sophia Ananiadou, and Yu Rong. 2022. Transformer for Graphs: An Overview from Architecture Perspective. *arXiv preprint arXiv:2202.08455* (2022).
- [33] Federico Monti, Davide Boscaini, Jonathan Masci, Emanuele Rodolà, Jan Svoboda, and Michael M. Bronstein. 2017. Geometric Deep Learning on Graphs and Manifolds Using Mixture Model CNNs. In *CVPR*. 5425–5434.
- [34] Fragkiskos Papadopoulos, Rodrigo Aldecoa, and Dmitri Krioukov. 2015. Network geometry inference using common neighbors. *Physical Review E* 92, 2 (2015), 022807.
- [35] Jiezhong Qiu, Yuxiao Dong, Hao Ma, Jian Li, Kuansan Wang, and Jie Tang. 2018. Network Embedding as Matrix Factorization: Unifying DeepWalk, LINE, PTE, and node2vec. In *WSDM*. 459–467.
- [36] Yu Rong, Wenbing Huang, Tingyang Xu, and Junzhou Huang. 2020. DropEdge: Towards Deep Graph Convolutional Networks on Node Classification. In *ICLR*.
- [37] Purnamrita Sarkar, Deepayan Chakrabarti, and Andrew W. Moore. 2010. Theoretical Justification of Popular Link Prediction Heuristics. In *COLT*. 295–307.
- [38] Prithviraj Sen, Galileo Namata, Mustafa Bilgic, Lise Getoor, Brian Gallagher, and Tina Eliassi-Rad. 2008. Collective Classification in Network Data. *AI Mag.* 29, 3 (2008), 93–106.
- [39] Oleksandr Shchur, Maximilian Mumme, Aleksandar Bojchevski, and Stephan Günnemann. 2018. Pitfalls of Graph Neural Network Evaluation. *CoRR abs/1811.05868* (2018).
- [40] Ashish Vaswani, Noam Shazeer, Niki Parmar, Jakob Uszkoreit, Llion Jones, Aidan N. Gomez, Lukasz Kaiser, and Illia Polosukhin. 2017. Attention is All you Need. In *NeurIPS*. 5998–6008.
- [41] Petar Veličković, Guillem Cucurull, Arantxa Casanova, Adriana Romero, Pietro Liò, and Yoshua Bengio. 2018. Graph Attention Networks. In *ICLR*.
- [42] Guangtao Wang, Rex Ying, Jing Huang, and Jure Leskovec. 2021. Multi-hop Attention Graph Neural Networks. In *IJCAI*.
- [43] Xiao Wang, Houye Ji, Chuan Shi, Bai Wang, Yanfang Ye, Peng Cui, and Philip S. Yu. 2019. Heterogeneous Graph Attention Network. In *WWW*. 2022–2032.
- [44] Boris Weisfeiler and Andrei Leman. 1968. The reduction of a graph to canonical form and the algebra which appears therein. *NTI, Series 2*, 9 (1968), 12–16.
- [45] Felix Wu, Amauri H. Souza Jr., Tianyi Zhang, Christopher Fifty, Tao Yu, and Kilian Q. Weinberger. 2019. Simplifying Graph Convolutional Networks. In *ICML*, Vol. 97. 6861–6871.
- [46] Zhanghao Wu, Paras Jain, Matthew Wright, Azalia Mirhoseini, Joseph E Gonzalez, and Ion Stoica. 2021. Representing long-range context for graph neural networks with global attention. In *NeurIPS*, Vol. 34. 13266–13279.
- [47] Kelvin Xu, Jimmy Ba, Ryan Kiros, Kyunghyun Cho, Aaron Courville, Ruslan Salakhudinov, Rich Zemel, and Yoshua Bengio. 2015. Show, attend and tell: Neural image caption generation with visual attention. In *ICML*. 2048–2057.
- [48] Keyulu Xu, Weihua Hu, Jure Leskovec, and Stefanie Jegelka. 2019. How Powerful are Graph Neural Networks?. In *ICLR*.
- [49] Keyulu Xu, Chengtao Li, Yonglong Tian, Tomohiro Sonobe, Ken-ichi Kawarabayashi, and Stefanie Jegelka. 2018. Representation Learning on Graphs with Jumping Knowledge Networks. In *ICML*, Vol. 80. 5449–5458.
- [50] Zhilin Yang, William Cohen, and Ruslan Salakhudinov. 2016. Revisiting semi-supervised learning with graph embeddings. In *ICML*. 40–48.
- [51] Chengxuan Ying, Tianle Cai, Shengjie Luo, Shuxin Zheng, Guolin Ke, Di He, Yanming Shen, and Tie-Yan Liu. 2021. Do Transformers Really Perform Badly for Graph Representation?. In *NeurIPS*. 28877–28888.

- [52] Jiaxuan You, Rex Ying, and Jure Leskovec. 2019. Position-aware Graph Neural Networks. In *ICML*, Vol. 97. 7134–7143.
- [53] Jiaxuan You, Zhitao Ying, and Jure Leskovec. 2020. Design Space for Graph Neural Networks. In *NeurIPS*.
- [54] Hanqing Zeng, Muhan Zhang, Yinglong Xia, Ajitesh Srivastava, Andrey Malevich, Rajgopal Kannan, Viktor Prasanna, Long Jin, and Ren Chen. 2021. Decoupling the depth and scope of graph neural networks. In *NeurIPS*, Vol. 34. 19665–19679.
- [55] Hanqing Zeng, Hongkuan Zhou, Ajitesh Srivastava, Rajgopal Kannan, and Viktor K. Prasanna. 2020. GraphSAINT: Graph Sampling Based Inductive Learning Method. In *ICLR*.
- [56] Kai Zhang, Yaokang Zhu, Jun Wang, and Jie Zhang. 2020. Adaptive Structural Fingerprints for Graph Attention Networks. In *ICLR*.
- [57] Qingru Zhang, David Wipf, Quan Gan, and Le Song. 2021. A Biased Graph Neural Network Sampler with Near-Optimal Regret. In *NeurIPS*. 8833–8844.
- [58] Shengzhong Zhang, Zengfeng Huang, Haicang Zhou, and Ziang Zhou. 2020. SCE: Scalable Network Embedding from Sparsest Cut. In *KDD*. 257–265.
- [59] Shuo Zhang and Lei Xie. 2020. Improving attention mechanism in graph neural networks via cardinality preservation. In *IJCAI*, Vol. 2020. 1395.
- [60] Jialin Zhao, Yuxiao Dong, Ming Ding, Evgeny Kharlamov, and Jie Tang. 2021. Adaptive Diffusion in Graph Neural Networks. In *NeurIPS*. 23321–23333.
- [61] Cheng Zheng, Bo Zong, Wei Cheng, Dongjin Song, Jingchao Ni, Wenchao Yu, Haifeng Chen, and Wei Wang. 2020. Robust Graph Representation Learning via Neural Sparsification. In *ICML*, Vol. 119. 11458–11468.

APPENDICES

A IRRELEVANCE BETWEEN CONNECTED NODES

In this section, we show a large amount of neighbors are found to highly differ regarding either node features or graph structure. The corresponding results obtained from Cora and Cite are exemplified here to demonstrate such phenomenon (Fig. 4 and 5).

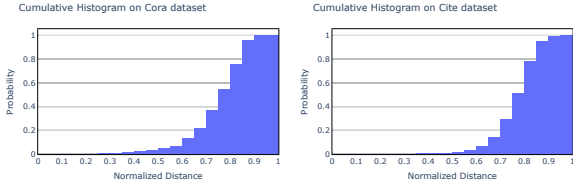


Figure 4: Cumulative histograms of normalized Euclidean distance regarding node features. Large values mean connected node pairs have very different features. Here most distances are large.

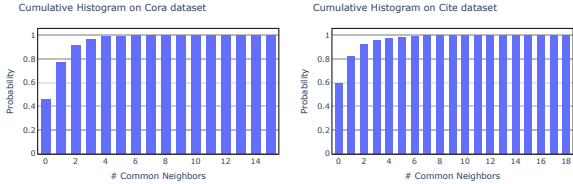


Figure 5: Cumulative histograms of common neighbors between connected node pairs. Small values mean connected node pairs differ in terms of graph structure. Here most values are 0s or close to 0.

The difference between the node features of connected nodes is measured by normalized Euclidean distance, with Fig. 4 depicting its cumulative histograms. It is evident that the distances of most node pairs in both datasets are very close to the largest. Specifically, the normalized distance of more than 70% of connected nodes in both datasets is higher than 0.7. This indicates that connected nodes have quite different features from their neighbors, and thus are highly irrelevant regarding node features.

The number of common neighbors is applied to measure the difference in the structure of connected nodes, with Fig. 5 depicting its cumulative histograms. The number of common neighbors is a widely used method to measure the similarity of two connected nodes [34, 37]. It is observed that around 50% of connected node pairs do NOT have even one common neighbor in Cora and Cite, and most connected node pairs (about 90%) have very few (0, 1 or 2) common neighbors. Thus, the structure of connected node pairs is highly different, indicating these nodes are very irrelevant.

Such observations indicate that a large portion of neighbors are irrelevant to the central node. These neighbors are possibly less informative for feature aggregation. Thus, they should be ignored by some appropriate attention mechanisms. Motivated by the discovered phenomenon that most neighbors are highly irrelevant, we propose Selective Attention to endow graph neural networks with the capability of flexibly ignoring irrelevant neighbors that can be identified by diverse forms of node-node dissimilarity.

B MORE DETAILS ON EXPERIMENTS

B.1 Data

Data description. The dataset statistics can be found in Table 1. Cora, Cite, and Pubmed are citation networks, where nodes, edges, and node features respectively represent the documents, document-document citations, and the keywords of the documents. Wiki and Uai are two web networks, where nodes, edges and node features represent web pages, web-web hyperlinks and descriptive information on these web pages, respectively. CoauthorCS is a co-authorship graph, where nodes are authors, which are connected by an edge if they co-author a paper, node features represent keywords for each author’s papers, and class labels indicate the most active fields of study for each author. For Cora, Cite and Pubmed, we follow previous works [22, 41] to use 20 nodes from each label as the training set, 500 nodes as the validation set, and 1000 nodes as the test set. For Wiki, Uai, and CoauthorCS, as there are no established splits for training and testing, we randomly generate five sets of splits. In each of them, 20 nodes of each ground truth class are sampled for training, 500 nodes are sampled for validation, and 1000 nodes are done for testing. For each of them, we randomly generate five sets of splits (i.e., training, validation, and testing splits) for the classification tasks, and use all nodes in each dataset for clustering tasks.

Pre-processing. From Table 1, we find the dimension of input features are too high in Wiki, Uai and CoauthorCS, which may cause unstable training performances. Thus we apply a trainable linear layer without non-linearity activation to reduce the feature dimensions. After the linear layer, the dimension of the input to the GNNs are reduced to 512. This pre-processing step is applied for both our models and all the baselines.

B.2 Detailed settings of all approaches

SATs are compared with twelve strong graph neural networks, including MoNet [33], GCN [22], GraphSage [13], JKNet [49], APPNP [23], ARMA [2], GIN [48], Neural Sparse [61], GAT [41], GATv2 [3], CAT [15], and HardGAT [10].

To perform unbiased comparisons, the source codes released by the authors are used to implement all the mentioned baselines. In our experiments, all the baselines use a two-layer network structure to learn node representations, meaning that the output layer of each GNN is followed by one hidden layer. As for the tuning of each baseline, we mainly follow the configurations presented in [15, 22, 41]. The configurations of the proposed SATs are generally same to those of GAT. Specifically, 8 attention heads are used in hidden layers, while the number of hidden layer dimension (for one head) is 8 for Cora, Cite, and Pubmed, and 32 for Wiki, Uai, and CoauthorCS. For the output layer, 1 attention head is used. “LeakyReLU” is used as the non-linearity in the attention mechanism with the negative slope as 0.2. All attention-based GNNs are trained with learning rate as 0.005, weight decay as 0.0005, number of training epochs as 1000 and dropout ratio as 0.6. For *Contractive apprehension span*, $\beta = 1.0$, while for *Subtractive apprehension span*, $\beta = 0.5$. All GNNs are initialized with Glorot initialization [11], and all GNNs are trained to minimize the cross-entropy loss of the training nodes using Adam optimizer [21]. All the experiments are

conducted on an NVIDIA RTX 3090 graphics card. The software environment of the experiments is CUDA 11.1, Python 3.8, and PyTorch 1.8.1.

B.3 Visualization of attention scores

We show the histograms of attention scores from the output layers of GAT, CAT and SATs in Fig. 6-11. It is not surprising that the attention coefficients learned by different variants of SAT are generally more concentrated. We observe that SAT is able to learn ignoring on Cora, Cite, Wiki and Uai datasets. SAT ignores fewer neighbors in citation networks, as Cora, Cite, and Pubmed are three very sparse graphs, which means there are few nodes having many neighbors, so SAT does not have enough training samples to learn ignoring. However, things are different on Wiki and Uai datasets, where there are much more very small attention values, which indicates SAT indeed learns to ignore irrelevant neighbors. It is obvious that learning-to-ignore is indeed the reason that SATs achieve state-of-the-art performances on all the testing datasets.

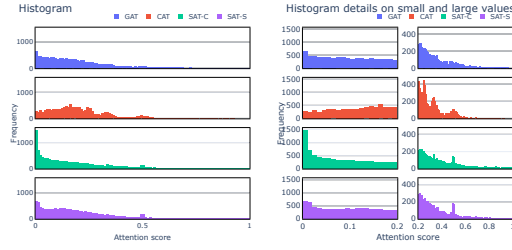


Figure 6: Attention scores from GAT, CAT and SAT on Cora

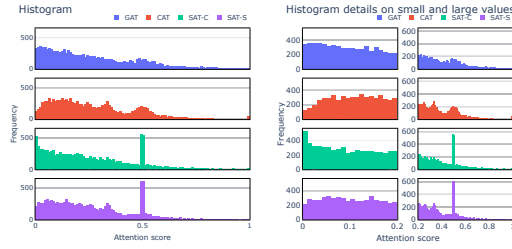


Figure 7: Attention scores from GAT, CAT and SAT on Cite

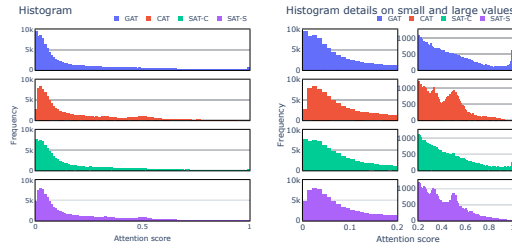


Figure 8: Attention scores from GAT, CAT and SAT on Pubmed

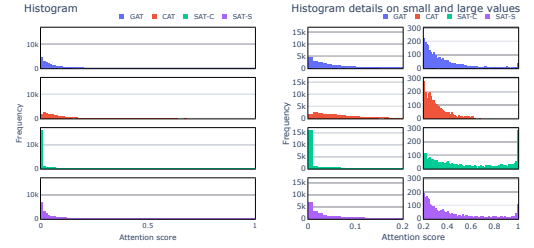


Figure 9: Attention scores from GAT, CAT and SAT on Wiki

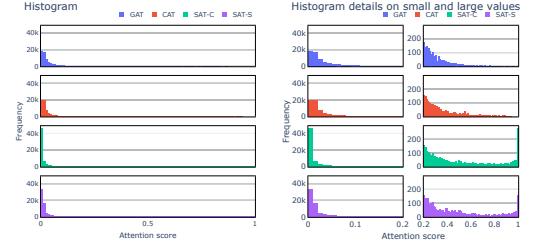


Figure 10: Attention scores from GAT, CAT and SAT on Uai

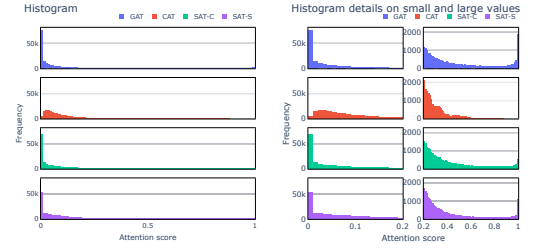


Figure 11: Attention scores from GAT, CAT and SAT on CoauthorCS

SUPPLEMENTARY MATERIALS

PROOFS OF EXPRESSIVE POWER

Proof of Theorem 4.1

PROOF. The proof of Theorem 4.1 can be divided into two parts, i.e., the proof of the sufficiency and necessity of the iff conditions [15, 48, 59]. The sufficiency of the iff conditions stated in Theorem 4.1 is firstly proved. Given a central node c_i , its aggregation function $h(c_i, X_i)$ can be written as:

$$h(c_i, X_i) = \sum_{x \in X_i} \alpha_{c_i x} g(x), \alpha_{c_i x} = \frac{f_{c_i x} \cdot d_{c_i x}}{\sum_{x \in X_i} f_{c_i x} \cdot d_{c_i x}}, \quad (9)$$

$$f_{c_i x} = \frac{\exp(m_{c_i x})}{\sum_{x \in X_i} \exp(m_{c_i x})}, d_{c_i x} = \exp(-\beta S_{c_i x}),$$

where $m_{c_i x}$ is the feature correlations between c_i and the neighbor having vectorized features x . Given Eq. (9), for two central nodes c_1 and c_2 , $h(c_1, X_1)$ and $h(c_2, X_2)$ can be written as:

$$h(c_1, X_1) = \sum_{x \in X_1} \alpha_{c_1 x} g(x) = \sum_{x \in X_1} \left[\frac{f_{c_1 x} \cdot d_{c_1 x}}{\sum_{x \in X_1} f_{c_1 x} \cdot d_{c_1 x}} \right] \cdot g(x)$$

$$h(c_2, X_2) = \sum_{x \in X_2} \alpha_{c_2 x} g(x) = \sum_{x \in X_2} \left[\frac{f_{c_2 x} \cdot d_{c_2 x}}{\sum_{x \in X_2} f_{c_2 x} \cdot d_{c_2 x}} \right] \cdot g(x) \quad (10)$$

If $M_1 = M_2$, $h(c_2, X_2)$ can be written as follows:

$$h(c_2, X_2) = \sum_{x \in M_2} \left[\frac{f_{c_2 x} \cdot \sum_{y=x, y \in X_2} d_{c_2 y}}{\sum_{x \in M_2} f_{c_2 x} \cdot \sum_{y=x, y \in X_2} d_{c_2 y}} \right] \cdot g(x)$$

$$= \sum_{x \in M_2} \left[\frac{\frac{\exp(m_{c_2 x})}{\sum_{x \in X_2} \exp(m_{c_2 x})} \cdot \sum_{y=x, y \in X_2} d_{c_2 y}}{\frac{\exp(m_{c_2 x})}{\sum_{x \in X_2} \exp(m_{c_2 x})} \cdot \sum_{y=x, y \in X_2} d_{c_2 y}} \right] \cdot g(x)$$

$$= \sum_{x \in M_2} \frac{\exp(m_{c_2 x}) \sum_{y=x, y \in X_2} \exp(-\beta S_{c_2 y})}{\sum_{x \in M_2} \exp(m_{c_2 x}) \sum_{y=x, y \in X_2} \exp(-\beta S_{c_2 y})} \cdot g(x). \quad (11)$$

Given $q \cdot \sum_{y=x, y \in X_1} \psi(-\beta S_{c_1 y}) = \sum_{y=x, y \in X_2} \psi(-\beta S_{c_2 y})$, and let $\psi(\cdot) \doteq \exp(\cdot)$, we have:

$$h(c_2, X_2) = \sum_{x \in M_1} \frac{q \cdot \exp(m_{c_2 x}) \sum_{y=x, y \in X_1} d_{c_1 y}}{\sum_{x \in M_1} q \cdot \exp(m_{c_2 x}) \sum_{y=x, y \in X_1} d_{c_1 y}} \cdot g(x). \quad (12)$$

$h(c_1, X_1) = h(c_2, X_2)$ can be derived if $c_1 = c_2$.

We next prove the necessity of the iff conditions that are stated in Theorem 4.1. And it can be achieved by showing possible contradictions when the iff conditions are not satisfied. If $h(c_1, X_1) = h(c_2, X_2)$, we have:

$$h(c_1, X_1) - h(c_2, X_2) =$$

$$\sum_{x \in X_1} \left[\frac{f_{c_1 x} \cdot d_{c_1 x}}{\sum_{x \in X_1} f_{c_1 x} \cdot d_{c_1 x}} \right] \cdot g(x)$$

$$- \sum_{x \in X_2} \left[\frac{f_{c_2 x} \cdot d_{c_2 x}}{\sum_{x \in X_2} f_{c_2 x} \cdot d_{c_2 x}} \right] \cdot g(x) = 0. \quad (13)$$

Firstly assuming $M_1 \neq M_2$, we thus have:

$$h(c_1, X_1) - h(c_2, X_2) =$$

$$\sum_{x \in M_1 \cap M_2} \left[\frac{\exp(m_{c_1 x}) \sum_{y=x, y \in X_1} d_{c_1 y}}{\sum_{x \in M_1} \exp(m_{c_1 x}) \sum_{y=x, y \in X_1} d_{c_1 y}} \right. \\ \left. - \frac{\exp(m_{c_2 x}) \sum_{y=x, y \in X_2} d_{c_2 y}}{\sum_{x \in M_2} \exp(m_{c_2 x}) \sum_{y=x, y \in X_2} d_{c_2 y}} \right] \cdot g(x)$$

$$+ \sum_{x \in M_1 \setminus M_2} \left[\frac{\exp(m_{c_1 x}) \sum_{y=x, y \in X_1} d_{c_1 y}}{\sum_{x \in M_1} \exp(m_{c_1 x}) \sum_{y=x, y \in X_1} d_{c_1 y}} \right] \cdot g(x)$$

$$- \sum_{x \in M_2 \setminus M_1} \left[\frac{\exp(m_{c_2 x}) \sum_{y=x, y \in X_2} d_{c_2 y}}{\sum_{x \in M_2} \exp(m_{c_2 x}) \sum_{y=x, y \in X_2} d_{c_2 y}} \right] \cdot g(x) = 0. \quad (14)$$

As Eq. (14) holds for any possible $g(\cdot)$, we define a new function $g'(\cdot)$:

$$g(x) = g'(x), \text{ for } x \in M_1 \cap M_2$$

$$g(x) = g'(x) - 1, \text{ for } x \in M_1 \setminus M_2 \quad (15)$$

$$g(x) = g'(x) + 1, \text{ for } x \in M_2 \setminus M_1$$

It is known that Eq. (14) holds for both $g(\cdot)$ and $g'(\cdot)$. Thus, we have:

$$h(c_1, X_1) - h(c_2, X_2) = 0 =$$

$$\sum_{x \in M_1 \cap M_2} \left[\frac{\exp(m_{c_1 x}) \sum_{y=x, y \in X_1} d_{c_1 y}}{\sum_{x \in M_1} \exp(m_{c_1 x}) \sum_{y=x, y \in X_1} d_{c_1 y}} \right. \\ \left. - \frac{\exp(m_{c_2 x}) \sum_{y=x, y \in X_2} d_{c_2 y}}{\sum_{x \in M_2} \exp(m_{c_2 x}) \sum_{y=x, y \in X_2} d_{c_2 y}} \right] \cdot g'(x)$$

$$+ \sum_{x \in M_1 \setminus M_2} \left[\frac{\exp(m_{c_1 x}) \sum_{y=x, y \in X_1} d_{c_1 y}}{\sum_{x \in M_1} \exp(m_{c_1 x}) \sum_{y=x, y \in X_1} d_{c_1 y}} \right] \cdot g'(x)$$

$$- \sum_{x \in M_2 \setminus M_1} \left[\frac{\exp(m_{c_2 x}) \sum_{y=x, y \in X_2} d_{c_2 y}}{\sum_{x \in M_2} \exp(m_{c_2 x}) \sum_{y=x, y \in X_2} d_{c_2 y}} \right] \cdot g'(x) \quad (16)$$

As Eqs. (14) and (16) are equal to zero, we have:

$$\sum_{x \in M_1 \setminus M_2} \left[\frac{\exp(m_{c_1 x}) \sum_{y=x, y \in X_1} d_{c_1 y}}{\sum_{x \in M_1} \exp(m_{c_1 x}) \sum_{y=x, y \in X_1} d_{c_1 y}} \right]$$

$$+ \sum_{x \in M_2 \setminus M_1} \left[\frac{\exp(m_{c_2 x}) \sum_{y=x, y \in X_2} d_{c_2 y}}{\sum_{x \in M_2} \exp(m_{c_2 x}) \sum_{y=x, y \in X_2} d_{c_2 y}} \right] = 0. \quad (17)$$

It is seen that Eq. (17) does not hold as $\exp(\cdot)$ is positive. $M_1 \neq M_2$ is therefore not true. Now assuming $M_1 = M_2 = M$ and excluding the irrational terms, Eq. (14) can be rewritten as follows:

$$\sum_{x \in M_1 \cap M_2} \left[\frac{\exp(m_{c_1 x}) \sum_{y=x, y \in X_1} d_{c_1 y}}{\sum_{x \in M_1} \exp(m_{c_1 x}) \sum_{y=x, y \in X_1} d_{c_1 y}} \right. \\ \left. - \frac{\exp(m_{c_2 x}) \sum_{y=x, y \in X_2} d_{c_2 y}}{\sum_{x \in M_2} \exp(m_{c_2 x}) \sum_{y=x, y \in X_2} d_{c_2 y}} \right] \cdot g(x) = 0. \quad (18)$$

To ensure the equation above to hold, each term in it has to be zero:

$$\frac{\exp(m_{c_1 x}) \sum_{y=x, y \in X_1} d_{c_1 y}}{\sum_{x \in M_1} \exp(m_{c_1 x}) \sum_{y=x, y \in X_1} d_{c_1 y}}$$

$$- \frac{\exp(m_{c_2 x}) \sum_{y=x, y \in X_2} d_{c_2 y}}{\sum_{x \in M_2} \exp(m_{c_2 x}) \sum_{y=x, y \in X_2} d_{c_2 y}} = 0. \quad (19)$$

The above equation can be further rewritten as:

$$\frac{\sum_{y=x, y \in X_1} d_{c_1 y}}{\sum_{y=x, y \in X_2} d_{c_2 y}} = \frac{\exp(m_{c_2 x}) \sum_{x \in M_1} \exp(m_{c_1 x}) \sum_{y=x, y \in X_1} d_{c_1 y}}{\exp(m_{c_1 x}) \sum_{x \in M_2} \exp(m_{c_2 x}) \sum_{y=x, y \in X_2} d_{c_2 y}}. \quad (20)$$

Assuming $M = \{s, s_0\}$, $c_1 = s_0$, $c_2 = s$, the feature correlations between the central node and its neighbors are $m_{c_1 x} = 1$ for $x \in M$, $m_{c_2 s} = 1$, and $m_{c_2 s_0} = 2$. When $x = s$, we have:

$$\frac{\sum_{s \in X_1} d_{c_1 s}}{\sum_{s \in X_2} d_{c_2 s}} = \frac{e[e \sum_{s \in X_1} d_{c_1 s} + e \sum_{s_0 \in X_1} d_{c_1 s_0}]}{e[e \sum_{s \in X_2} d_{c_2 s} + e^2 \sum_{s_0 \in X_2} d_{c_2 s_0}]}. \quad (21)$$

$d_{cx} = \exp(-\beta S_{cx})$ can be any positive value as the computation of feature correlation and the learning of node-node dissimilarity (S) are mutually independent. Considering $d_{cx} = \exp(-\beta S_{cx}) = a > 0$, we have $\frac{\mu_1(s)}{\mu_2(s)} = \frac{|X_1|}{|X_2| - n + ne}$. This equation does not hold because LHS (a rational number) does not equal RHS (an irrational number). Thus, $c_1 \neq c_2$ is not true. Let $c_1 = c_2 = c$, Eq. (20) can be rewritten as follows:

$$\frac{\sum_{y=x, y \in X_1} d_{cy}}{\sum_{y=x, y \in X_2} d_{cy}} = \frac{\sum_{x \in M_1} \exp(m_{cx}) \sum_{y=x, y \in X_1} d_{cy}}{\sum_{x \in M_2} \exp(m_{cx}) \sum_{y=x, y \in X_2} d_{cy}} = \text{const} > 0. \quad (22)$$

Setting $\frac{1}{q} = \text{const}$ and $d_{cy} = \exp(-\beta S_{cy}) = \psi(-\beta S_{cy})$, we finally have $q \sum_{y=x, y \in X_1} \psi(-\beta S_{cy}) = \sum_{y=x, y \in X_2} \psi(-\beta S_{cy})$. \square

Proof of Theorem 4.2

PROOF. Theorem 4.2 can also be proved by considering the sufficiency and necessity of the iff conditions stated. The sufficiency of the iff conditions in Theorem 4.2 is firstly proved. Given a central node c_i , its aggregation function $h(c_i, X_i)$ can be written as:

$$h(c_i, X_i) = \sum_{x \in X_i} \alpha_{c_i x} g(x), \alpha_{c_i x} = \frac{f_{c_i x} \cdot d_{c_i x}}{\sum_{x \in X_i} f_{c_i x} \cdot d_{c_i x}}, \quad (23)$$

$$f_{c_i x} = \frac{\exp(m_{c_i x})}{\sum_{x \in X_i} \exp(m_{c_i x})}, d_{c_i x} = 1 - \beta \frac{\exp(S_{c_i x})}{\sum_{x \in X_i} \exp(S_{c_i x})},$$

Given $c_1 = c_2$, $M_1 = M_2 = M$, $q[\sum_{y=x, y \in X_1} \sum_{x \in X_1} \psi(S_{c_1 x}) - \sum_{y=x, y \in X_1} \beta \psi(S_{c_1 y})] = \sum_{y=x, y \in X_2} \sum_{x \in X_2} \psi(S_{c_2 x}) - \sum_{y=x, y \in X_2} \beta \psi(S_{c_2 y})$, and $\psi(\cdot) \doteq \exp(\cdot)$, we have:

$$h(c_2, X_2) = \sum_{x \in X_2} \frac{f_{c_2 x} \cdot d_{c_2 x}}{\sum_{x \in X_2} f_{c_2 x} \cdot d_{c_2 x}} g(x)$$

$$= \sum_{x \in M_2} \frac{\exp(m_{c_2 x}) \sum_{y=x, y \in X_2} [1 - \beta \frac{\exp(S_{c_2 y})}{\sum_{y \in X_2} \exp(S_{c_2 y})}]}{\sum_{x \in M_2} \exp(m_{c_2 x}) \sum_{y=x, y \in X_2} [1 - \beta \frac{\exp(S_{c_2 y})}{\sum_{y \in X_2} \exp(S_{c_2 y})}]} g(x)$$

$$= \sum_{x \in M_1} \frac{q \cdot \exp(m_{c_1 x}) \sum_{y=x, y \in X_1} d_{c_1 y}}{\sum_{x \in M_1} q \cdot \exp(m_{c_1 x}) \sum_{y=x, y \in X_1} d_{c_1 y}} g(x) = h(c_1, X_1). \quad (24)$$

Next, we prove the necessity of the iff conditions stated in Theorem 4.2. Given $h(c_1, X_1) = h(c_2, X_2)$, we have:

$$h(c_1, X_1) - h(c_2, X_2) = \sum_{x \in X_1} \left[\frac{f_{c_1 x} \cdot d_{c_1 x}}{\sum_{x \in X_1} f_{c_1 x} \cdot d_{c_1 x}} \right] \cdot g(x) - \sum_{x \in X_2} \left[\frac{f_{c_2 x} \cdot d_{c_2 x}}{\sum_{x \in X_2} f_{c_2 x} \cdot d_{c_2 x}} \right] \cdot g(x) = 0. \quad (25)$$

Assuming $M_1 \neq M_2$, we have:

$$h(c_1, X_1) - h(c_2, X_2) = \sum_{x \in M_1 \cap M_2} \left[\frac{\exp(m_{c_1 x}) \sum_{y=x, y \in X_1} d_{c_1 y}}{\sum_{x \in M_1} \exp(m_{c_1 x}) \sum_{y=x, y \in X_1} d_{c_1 y}} - \frac{\exp(m_{c_2 x}) \sum_{y=x, y \in X_2} d_{c_2 y}}{\sum_{x \in M_2} \exp(m_{c_2 x}) \sum_{y=x, y \in X_2} d_{c_2 y}} \right] \cdot g(x) + \sum_{x \in M_1 \setminus M_2} \left[\frac{\exp(m_{c_1 x}) \sum_{y=x, y \in X_1} d_{c_1 y}}{\sum_{x \in M_1} \exp(m_{c_1 x}) \sum_{y=x, y \in X_1} d_{c_1 y}} \right] \cdot g(x) - \sum_{x \in M_2 \setminus M_1} \left[\frac{\exp(m_{c_2 x}) \sum_{y=x, y \in X_2} d_{c_2 y}}{\sum_{x \in M_2} \exp(m_{c_2 x}) \sum_{y=x, y \in X_2} d_{c_2 y}} \right] \cdot g(x) = 0. \quad (26)$$

Again we may define $g'(\cdot)$ as Eq. (15) shows. It is known that $h(c_1, X_1) - h(c_2, X_2) = 0$ holds for both $g(\cdot)$ and $g'(\cdot)$. Thus, we have:

$$h(c_1, X_1) - h(c_2, X_2) = \sum_{x \in M_1 \cap M_2} \left[\frac{\exp(m_{c_1 x}) \sum_{y=x, y \in X_1} d_{c_1 y}}{\sum_{x \in M_1} \exp(m_{c_1 x}) \sum_{y=x, y \in X_1} d_{c_1 y}} - \frac{\exp(m_{c_2 x}) \sum_{y=x, y \in X_2} d_{c_2 y}}{\sum_{x \in M_2} \exp(m_{c_2 x}) \sum_{y=x, y \in X_2} d_{c_2 y}} \right] \cdot g'(x) + \sum_{x \in M_1 \setminus M_2} \left[\frac{\exp(m_{c_1 x}) \sum_{y=x, y \in X_1} d_{c_1 y}}{\sum_{x \in M_1} \exp(m_{c_1 x}) \sum_{y=x, y \in X_1} d_{c_1 y}} \right] \cdot g'(x) - \sum_{x \in M_2 \setminus M_1} \left[\frac{\exp(m_{c_2 x}) \sum_{y=x, y \in X_2} d_{c_2 y}}{\sum_{x \in M_2} \exp(m_{c_2 x}) \sum_{y=x, y \in X_2} d_{c_2 y}} \right] \cdot g'(x) = 0. \quad (27)$$

As both Eqs. (26) and (27) equal zero, we have:

$$\sum_{x \in M_1 \setminus M_2} \left[\frac{\exp(m_{c_1 x}) \sum_{y=x, y \in X_1} d_{c_1 y}}{\sum_{x \in M_1} \exp(m_{c_1 x}) \sum_{y=x, y \in X_1} d_{c_1 y}} \right] + \sum_{x \in M_2 \setminus M_1} \left[\frac{\exp(m_{c_2 x}) \sum_{y=x, y \in X_2} d_{c_2 y}}{\sum_{x \in M_2} \exp(m_{c_2 x}) \sum_{y=x, y \in X_2} d_{c_2 y}} \right] = 0. \quad (28)$$

Like the analysis on proving Theorem 4.1, $M_1 \neq M_2$ is false. Now we are able to assume $M_1 = M_2 = M$. The terms about $x \in M_1 \setminus M_2$ and $x \in M_2 \setminus M_1$ in Eq. (26) can therefore be eliminated and it is known that the following equation must hold to ensure $h(c_1, X_1) - h(c_2, X_2) = 0$:

$$\frac{\sum_{y=x, y \in X_1} d_{c_1 y}}{\sum_{y=x, y \in X_2} d_{c_2 y}} = \frac{\exp(m_{c_2 x}) \sum_{x \in M_1} \exp(m_{c_1 x}) \sum_{y=x, y \in X_1} d_{c_1 y}}{\exp(m_{c_1 x}) \sum_{x \in M_2} \exp(m_{c_2 x}) \sum_{y=x, y \in X_2} d_{c_2 y}}. \quad (29)$$

Assuming $M = \{s, s_0\}$, $c_1 = s_0$, $c_2 = s$, the feature correlations between the central node and its neighbors are $m_{c_1x} = 1$ for $x \in M$, $m_{c_2s} = 1$, and $m_{c_2s_0} = 2$. When $x = s$, we have:

$$\frac{\sum_{s \in X_1} d_{c_1s}}{\sum_{s \in X_2} d_{c_2s}} = \frac{e[e \sum_{s \in X_1} d_{c_1s} + e \sum_{s_0 \in X_1} d_{c_1s_0}]}{e[e \sum_{s \in X_2} d_{c_2s} + e^2 \sum_{s_0 \in X_2} d_{c_2s_0}]}. \quad (30)$$

$d_{cx} = 1 - \beta \frac{\exp(S_{cx})}{\sum_{x \in X} \exp(S_{cx})}$ can be any positive value as the computation of feature correlation and the learning of S are mutually independent. Considering $d_{cx} = a > 0$, We have $\frac{\mu_1(s)}{\mu_2(s)} = \frac{|X_1|}{|X_2|^{-n+ne}}$. This equation does not hold because LHS (a rational number) does not equal RHS (an irrational number). Thus, $c_1 \neq c_2$ is false. Since $c_1 = c_2 = c$, Eq. (29) can be rewritten as:

$$\begin{aligned} & \frac{\sum_{y=x, y \in X_1} [\sum_{x \in X_1} \exp(S_{cx}) - \beta \exp(S_{cy})]}{\sum_{y=x, y \in X_2} [\sum_{x \in X_2} \exp(S_{cx}) - \beta \exp(S_{cy})]} = \\ & \frac{\sum_{x \in M_1} \exp(m_{cx}) \sum_{y=x, y \in X_1} [\sum_{x \in X_1} \exp(S_{cx}) - \beta \exp(S_{cy})]}{\sum_{x \in M_2} \exp(m_{cx}) \sum_{y=x, y \in X_2} [\sum_{x \in X_2} \exp(S_{cx}) - \beta \exp(S_{cy})]} \\ & = \text{const} > 0. \end{aligned} \quad (31)$$

Letting $\text{const} = \frac{1}{q}$ and $\exp(\cdot) = \psi(\cdot)$, we finally have $q \sum_{y=x, y \in X_1} [\sum_{x \in X_1} \psi(S_{cx}) - \beta \psi(S_{cy})] = \sum_{y=x, y \in X_2} [\sum_{x \in X_2} \psi(S_{cx}) - \beta \psi(S_{cy})]$. \square

Proof of Corollary 4.3

PROOF. We may complete this proof by following the procedure presented in [15, 48]. According to Theorem 4.1, we assume $X_1 = (M, \mu_1)$, $X_2 = (M, \mu_2)$, $c \in M$, and $q \cdot \sum_{y=x, y \in X_1} \psi(-\beta S_{c_1y}) = \sum_{y=x, y \in X_2} \psi(-\beta S_{c_2y})$, for $q > 0$. When \mathcal{T} uses the attention scores solely according to Eq. (2) to aggregate node features, we have $\sum_{x \in X_1} \alpha_{cx}g(x) = \sum_{x \in X_2} \alpha_{cx}g(x)$. This means \mathcal{T} fails to discriminate the structures satisfying the conditions stated in Theorem 4.1. When \mathcal{T} uses Eq. (4) where the attention coefficients are obtained by the *Contractive apprehension span* (Eq. (2)) to aggregate node features, we have $\sum_{x \in X_1} \alpha_{cx}g(x) - \sum_{x \in X_2} \alpha_{cx}g(x) = \epsilon(\frac{1}{|X_1|} - \frac{1}{|X_2|})\alpha_{cc}g(c)$, where $|X_1| = |N_1|$, and $|X_2| = |N_2|$. Since $|X_1| \neq |X_2|$, $\sum_{x \in X_1} \alpha_{cx}g(x) - \sum_{x \in X_2} \alpha_{cx}g(x) \neq 0$, which means \mathcal{T} based on Eqs. (2) and (4) is able to discriminate all the structures that \mathcal{T} solely based on Eq. (2) fails to distinguish. Following the similar procedure, when the Selective Attention layer (Eq. (4)) utilizes the *Subtractive apprehension span* (Eq. (3)), we are able to prove that the corresponding aggregation function also can distinguish those distinct structures that the aggregation function only using *Subtractive apprehension span* fails to discriminate. \square